

## Nuclear envelope organization in papillary thyroid carcinoma

A.H. Fischer<sup>1</sup>, P. Taysavang<sup>1</sup>, C.J. Weber<sup>2</sup> and K.L. Wilson<sup>3</sup>

<sup>1</sup>Department of Pathology, <sup>2</sup>Department of Surgery, Emory University Hospital, Atlanta and <sup>3</sup>Department of Cell Biology and Anatomy, The Johns Hopkins University School of Medicine, Baltimore, USA

**Summary.** Papillary thyroid carcinomas (PTCs) have characteristic nuclear shape changes compared to follicular-type thyroid epithelium. We tested the hypothesis that the altered nuclear shape results from altered distribution or expression of the major structural proteins of the nuclear envelope. Lamin A, lamin B1, lamin C, lamin B receptor (LBR), lamina-associated polypeptide 2 (LAP2), emerin, and nuclear pores were examined. PTC's with typical nuclear features by H&E were compared to non-neoplastic thyroid and follicular neoplasms using confocal microscopy, and semi-quantitative immunoblotting. Lamin A/C, lamin B1, LAP2, emerin, and nuclear pores all extend throughout the grooves and intranuclear inclusions of PTC. Their distribution and fluorescent intensity is not predictably altered relative to nuclear envelope irregularities. By immunoblotting, the abundance (per cell) and electrophoretic mobilities of lamin A, lamin B1, lamin C, emerin, and LAP2 proteins do not distinguish PTC, normal thyroid, or follicular neoplasms. These results do not support previously published predictions that lamin A/C expression is related to a loss of proliferative activity. At least three LAP2 isoforms are identified in normal and neoplastic thyroid. LBR is sparse or undetectable in all the thyroid samples. The results suggest that the irregular nuclear shape of PTC is not determined by these nuclear envelope structural proteins *per se*. We review the structure of the nuclear envelope, the major factors that determine nuclear shape, and the possible functional consequences of its alteration in PTC.

**Key words:** Thyroid neoplasm, Nuclear envelope, Lamin

### Introduction

Normal thyroid epithelium can be transformed via

*Offprint requests to:* Andrew H. Fischer, M.D., Department of Pathology, UMASS Memorial Healthcare, University of Massachusetts, 55 Lake Ave North Worcester, MA 01655. Fax: 508-856-2968

two different pathways. The two pathways lead to papillary thyroid carcinoma (PTC) or follicular neoplasms. Papillary thyroid carcinoma is diagnosed largely on the basis of nuclear contour changes and changes in heterochromatin texture (Vickery et al., 1985). Both normal thyroid cells and follicular neoplasms tend to have rigidly spherical nuclear contours, and they generally have block-like aggregates of heterochromatin apposed to the nuclear envelope. In contrast, typical papillary thyroid carcinomas have fine, rather than block-like heterochromatin, and they exhibit frequent buckling of their nuclei with characteristic grooves and occasional rounded nuclear envelope invaginations termed intranuclear cytoplasmic inclusions (Rosai et al., 1992). The nuclear contour changes of papillary thyroid carcinoma can be appreciated in non-fixed living cells (AH Fischer, unpublished observations), after formalin, alcohol or air drying fixation, and by electron microscopy (Johannessen et al., 1983; Oyama, 1989; LiVolsi, 1990). The papillary thyroid carcinoma oncogene (RET/PTC), is active early in the formation of PTCs (Viglietto et al., 1995; Klugbauer et al., 1998), and appears sufficient to mediate the changes in nuclear envelope contour and heterochromatin characteristic of PTC (Fischer et al., 1998a). In contrast, activation of RAS (a frequent early event in the genesis of follicular neoplasms; Lemoine et al., 1989; reviewed in Wynford-Thomas, 1997), leaves the nucleus round and coarsens heterochromatin when expressed in either normal thyroid (Fischer et al., 1998a) or fibroblast cells (Fischer et al., 1998b).

A precise molecular understanding of the morphologic changes in cancer cell nuclei is a rational means of improving diagnosis. PTC provides an excellent model system. Since many forms of cancer besides PTC show nuclear contour abnormalities (Frost, 1986), a biochemical characterization of the nuclear contour changes could have broad diagnostic utility. In addition, defining the nuclear contour changes in biochemical terms would facilitate studies of the apparently divergent signaling pathways downstream of RET/PTC and RAS in the thyroid.

Nuclear contour is defined by the large scale

08 ENE. 2001



organization of the nuclear envelope. The nuclear envelope includes four major structural elements: the nuclear lamina, inner nuclear membrane, outer nuclear membrane, and nuclear pore complexes (reviewed in Gerace and Foisner, 1994; Moir et al., 1995; Gant and Wilson, 1997; Ohno et al., 1998). The nuclear lamina is situated between the inner nuclear membrane and chromatin; some of the proteins of the nuclear lamina are also present in the interior of the nucleus. In most cells, the peripheral nuclear lamina is too thin to be resolved by routine transmission electron microscopy. The nuclear lamina is a flexible, elastic yet strong (Maniotis et al., 1997; Heidemann et al., 1999) meshwork of protein fibers, composed primarily of polymerized nuclear-specific type V intermediate filament proteins called lamins. The abundance of the filamentous lamins has suggested a role in determining nuclear shape (reviewed in Moir et al., 1995). Accordingly, altered expression, or expression of mutant lamins can affect nuclear contour (Loewinger and McKeon, 1988; Furukawa and Hotta, 1993; Ellis et al., 1997; Lenz-Bohme et al., 1997). There are two classes of lamins. The A-type lamins include lamins A and C (~72 and 62 kD) which arise from differential splicing of the same transcript, followed by different post-translational modifications (reviewed by Moir et al., 1995). Expression of lamins A and C appears to be regulated at the level of both transcription and mRNA stability (Lanoix et al., 1992). There are two known human B-type lamin genes, named lamin B1 and B2. All mammalian cells express one or both of these lamins. Lamin B2 is known to be widely expressed, except in hepatocytes (Broers et al., 1997). The expression of lamins in PTC has not been studied.

The stable assembly of lamins at the nuclear periphery may be mediated by their binding to several relatively abundant integral membrane proteins restricted to the inner nuclear membrane (reviewed in Georgatos et al., 1994; Gerace and Foisner, 1994; Gant and Wilson, 1997). Since some of these membrane proteins also bind to chromatin, they are obvious candidates for mediating the large-scale changes in nuclear envelope and chromatin organization of PTC. The lamin B receptor or LBR (~58 kD) was so named because it binds lamin B with high affinity and is present at high concentration in the avian erythrocyte nuclear envelopes in which it was first characterized (Worman et al., 1988; reviewed in Ye et al., 1998). The tissue distribution of human LBR is incompletely characterized. LBR also may help organize large-scale chromatin distribution and transcription since it binds to a heterochromatin protein called Hp1 (Ye and Worman, 1996; Ye et al., 1997). Hp1 was originally identified as a mediator of position effect variegation in *Drosophila*, helping repress transcription. LBR may also function to target mitotic nuclear envelope vesicles back to the surface of chromosomes during post-mitotic nuclear envelope re-assembly (Pyrpasopoulou et al., 1996).

Two unrelated lamin-associated polypeptides

(LAPs), named LAP1 and LAP2, both have high affinity for lamin B (Foisner and Gerace, 1993). LAP1 may also bind weakly to lamins A/C (Foisner and Gerace, 1993; reviewed in Gerace and Foisner, 1994). The function and distribution of LAP1 is not well-characterized. More is known about LAP2, a protein with distinct chromatin and lamin B binding domains (Foisner and Gerace, 1993; Yang et al., 1997). LAP2 may bind chromatin via a small DNA-binding protein of unknown function named Barrier to Autointegration Factor (BAF) (Lee and Craigie, 1998; Furukawa, 1999). Humans express at least three major splicing isoforms of LAP2, named  $\alpha$ ,  $\beta$ , and  $\gamma$  (Harris et al., 1995; Berger et al., 1996) and possibly four minor isoforms, as identified in mice (Berger et al., 1996). LAP2 isoforms appear to regulate lamina re-assembly and nuclear envelope expansion after mitosis (Yang et al., 1997; Gant et al., 1999). The largest LAP2 isoform, LAP2 $\alpha$  (~75 kD), lacks a membrane spanning domain, and behaves biochemically as a component of the nuclear matrix by resisting extraction with detergent, nuclease and salt (Dechat et al., 1998). The status of LAP2 proteins has not been studied in relation to tumorigenesis, and it is not known if they are present in the thyroid.

Related to LAP2, and also located on the inner nuclear membrane, are two additional proteins named emerin (Manilal et al., 1996) and MAN1 (Paulin-Levasseur et al., 1996). Emerin was discovered because its loss causes the X-linked hereditary syndrome Emery-Dreifuss muscular dystrophy (EDMD), characterized clinically by contractures, slowly progressive muscle wasting, and cardiac conduction defects (Emery, 1989; reviewed in Morris and Manilal, 1999; Wilson, 2000). Emerin is widely expressed, but its presence in the thyroid has not been documented (Manilal et al., 1996). Curiously, an autosomal dominant form of EDMD, which has the same range of clinical symptoms as the X-linked form, is caused by dominant mutations in the lamin A/C gene (Bonne et al., 1999), suggesting possible overlapping functions downstream of these proteins. The mechanism by which loss of emerin or lamin A/C causes delayed degenerations in only certain cell types is not yet known. Emerin appears to interact with the lamina or chromatin (Manilal et al., 1996; reviewed in Wilson, 2000). Very little is yet known about the recently cloned MAN1 gene (Paulin-Levasseur et al., 1996; H. Worman, personal communication).

The outer nuclear envelope faces the cytoplasm and is proposed to interact with the cytoskeleton, although very little is known about the molecular basis for the interaction (Goldman et al., 1985; Georgatos and Blobel, 1987; Albers and Fuchs, 1989). The outer nuclear membrane is continuous with the endoplasmic reticulum. The inner and outer nuclear membranes join at the nuclear pore complexes. Nuclear pore complexes are bound to the nuclear lamina, perhaps via attachment with lamins (Dwyer and Blobel, 1976; Lenz-Bohme et al., 1997). An electron micrograph study demonstrated that the total number of nuclear pore complexes per cell

## Papillary thyroid carcinoma nuclear envelope

is decreased in PTCs even though the surface area of the nuclear envelope in PTCs was greater than in follicular samples (Johannessen et al., 1982). The distribution of nuclear pore complexes relative to grooves and inclusions has not been described.

The purpose of the present study was to broadly survey the organization of the nuclear envelope in PTC cells, and test the hypothesis that changes in the expression or distribution of the major nuclear envelope proteins are responsible for the diagnostic nuclear contour irregularity of PTC. Specifically, we asked if there was a predictable absence or over-expression of any of the major nuclear envelope structural proteins in the landmark grooves and inclusions in PTC. We also asked if the electrophoretic mobilities or relative abundance of lamins A, B1, C, LBR, LAP2 isoforms, or emerin were altered in PTC relative to control tissues.

### Materials and methods

#### Cases studied

The source of material for these studies was excess tissue not needed for diagnosis from surgically resected human thyroids, as approved by the Emory Human Investigations Committee. Table 1 lists the cases studied. Classification (by A. H. F.) follows the Armed Forces Institute of Pathology Fascicle (Rosai et al., 1992). By hematoxylin and eosin staining, the 14 PTCs all showed typical diagnostic nuclear features including nuclear contour irregularity, grooves and inclusions. Table 1 shows the tumor size, nodal status, and presence of metastatic disease (TNM status) (Beahrs et al., 1992) at the time the tissue was procured. Twelve of the 14 were "differentiated" and showed typical dispersed chromatin (Rosai et al., 1992). One of these twelve (PTC-9) had dedifferentiated in another area into an anaplastic thyroid carcinoma. Two tall cell variants of PTC were included. Follicular thyroid samples with typical relatively round nuclear contours by hematoxylin and eosin staining, served as controls. These follicular thyroid samples included adjacent normal thyroid tissue from three patients (without lymphocytic thyroiditis or nodular change), three follicular adenomas, one angio-invasive oncocytic carcinoma (Hurthle cell carcinoma), one angio-invasive well-differentiated follicular carcinoma, and four poorly differentiated follicular carcinomas. We classify these four poorly differentiated carcinomas as follicular-type neoplasms (Rosai et al., 1992) due to a combination of an absence of the nuclear features of PTC, absence of papillary architecture, and predominance of venous invasion over lymphatic invasion. Three of these are subclassified as insular carcinomas. One "well-differentiated thyroid carcinoma not otherwise specified" was diagnosed according to criteria in (Rosai et al., 1992). This tumor showed partially developed nuclear morphologic changes of PTC but was entirely follicular in architecture, was encapsulated, and showed venous but not lymphatic

invasion.

#### Fixation for immunofluorescence staining

Smears from the tumors or non-neoplastic thyroid were prepared by scraping the surface with one microscope slide, smearing the sample on a second slide, and immediately immersing in either 95% alcohol (Flex, Richard Allen, Kalamazoo, MI) or 10% normal buffered formalin (NBF) (Biochemical Sciences, Inc., Swedesboro, NJ) at room temperature. Smears were held indefinitely in 95% alcohol at 4 degrees before immunostaining. For NBF fixation, smears were transferred out of room temperature NBF after 15 minutes fixation and held at 4 degrees in phosphate buffered saline (PBS) for up to one week.

#### Antibodies

Rabbit polyclonal antibodies to lamin A/C and lamin B1 were a kind gift of Dr. Nilhabh Chaudhary. The lamin A/C antibody was raised against amino acids 413-426 of the human lamin A/C gene, corresponding to an epitope shared by both lamins A and C. The lamin B1 antibody was raised against amino acids 411-424, specific to human lamin B1. These antibodies have been previously characterized (Chaudhary and Courvalin, 1993; Hytiroglou et al., 1993), and were confirmed on immunoblots for this study: each sera specifically recognized proteins of the appropriate molecular weight that co-purify with hepatocyte and normal thyroid nuclear envelopes, prepared as described by Dwyer and Blobel, 1976. Both lamin antibodies were used at dilutions of 1:50 for immunofluorescence and 1:1000 for immunoblotting. A monoclonal mouse antibody reactive with emerin, clone 4G5 (Novo Castra laboratories, New Castle upon Tyne, UK) was used at 1:500 for immunofluorescence and 1:5000 for immunoblots. A mouse monoclonal antibody recognizing nuclear pore proteins, Mab414 (Berkeley Antibody Company, Richmond CA), was diluted 1:500 for immunofluorescence. Immunostaining of alcohol-fixed material could not be achieved with the 414 antibody. Therefore, all nuclear pore immunostaining was performed on formalin fixed smears. An affinity purified rabbit polyclonal antibody raised against the N-terminus of the human lamin B receptor (Ye and Worman, 1996), a generous gift of Dr. Howard Worman, Columbia University, was used at 1:500 dilution for immunoblotting. A polyclonal antiserum against human LAP2 was raised by immunizing rabbit #2804 with a bacterially-expressed purified His-tagged polypeptide consisting of N-terminal amino acids 1-187 of human LAP2. These amino acids are present in all three known human isoforms of LAP2 (Harris et al., 1995) and all seven mouse isoforms (Berger et al., 1996). Thus, the antibody is expected to detect all known isoforms of LAP2. This expectation was confirmed on immunoblots; serum #2804 reacted specifically with three major

proteins of the expected molecular weight (~76, 54, and 38 kD) from hepatocyte nuclei, and specifically stained the nuclear periphery by indirect immunofluorescence. Whole serum was used at dilutions of 1:10,000 for immunoblotting and 1:500 for immunofluorescence. Pre-immune serum from the same rabbit was totally non-reactive in paired control immunoblots and immunofluorescence experiments, even when used at concentrations ten times higher than immune serum.

Secondary antibodies for immunofluorescence (Jackson Immunoresearch Laboratory, West Grove, PA) included fluorescein isothiocyanate (FITC) conjugated goat anti-mouse Fab fragments (14  $\mu\text{g/ml}$ ), FITC-conjugated goat anti-rabbit whole IgG (15  $\mu\text{g/ml}$ ), Cy3 Donkey anti-rabbit Fab fragments (2.8  $\mu\text{g/ml}$ ), and Cy3 sheep anti-mouse Fab fragments (2.6  $\mu\text{g/ml}$ ). For immunoblotting, secondary antibodies (Amersham Life Sciences, Jackson Heights, IL) included horseradish peroxidase conjugated donkey anti-rabbit antibody at 1:1000 dilution, and horseradish peroxidase conjugated sheep anti-mouse antibody at 1:3000 dilution.

#### *Immunofluorescence staining protocol*

Smears were rinsed or rehydrated with PBS, then cells were permeabilized with 0.5% triton X-100 (Sigma) in PBS for 15 minutes at room temperature and rinsed three times with PBS. A 20 minute incubation at room temperature with 10% fetal calf serum (FCS) (Atlanta Biologicals, Norcross, GA) in PBS was performed to block non-specific binding. 100  $\mu\text{l}$  of primary antibody diluted into 10% FCS in PBS was layered onto the smears and covered with a glass coverslip for 1 hour at room temperature. Three washes with PBS was followed by incubation for 30 minutes at room temperature with 100  $\mu\text{l}$  of fluorescent secondary antibody in PBS with 1% FCS. Three washes with PBS was followed by incubation for 15 minutes in 10  $\mu\text{g/ml}$  propidium iodide in PBS at room temperature for most samples. After three final washes in PBS, smears were coverslipped with DAKO Fluorescent Mounting Medium (Carpenteria, CA).

#### *Confocal microscopy*

A Zeiss LSM 410 Confocal microscope with an Argon/Krypton laser was used to capture images using non-overlapping FITC (green, or yellow if superimposed on red) and propidium iodide or Cy3 (red) detection channels. A Zeiss 100 X oil immersion plan apochromat lens with a numerical aperture of 1.4 was used with a zoom setting of 3 for final magnification of 3000X. Pinhole settings of 18 were used, corresponding to a Z-plane thickness of 0.5 microns. For most work, serial images in the X-Y plane were collected at a spacing of 1 micrometer.

#### *Cell fractionation and immunoblotting*

All samples examined by immunoblotting were

studied in adjacent histologic sections to calculate the percent thyrocytes and percent mitotic cells in the sample. At least 200 randomly encountered cells were scored as either thyrocytes or non-epithelial cells (principally lymphocytes, fibroblasts and plasma cells). Most samples had more than 85% thyroid epithelial cells. Sample PTC-1 had approximately 50% non-epithelial cells, principally lymphocytes and plasma cells. All samples contained far fewer than 1% mitotic cells. Ploidy analysis by image analysis of feulgen stained smears, or flow cytometry was performed to validate the use of total DNA content in the cell lysates as a measure of cell number. All but four cases were diploid.

Snap frozen samples, stored at -70 °C, were broken under liquid nitrogen into 1-3 mm size fragments, then dounced with a tight fitting pestle in approximately 4 volumes of ice-cold TKM buffer (50 mM TRIS, 5 mM  $\text{MgCl}_2$ , 2.5 mM KCl, 0.23M sucrose, 6 mM  $\beta$ -mercaptoethanol) with freshly added protease inhibitors including 1 mM phenylmethylsulphonylfluoride, and 10  $\mu\text{g/ml}$  each of aprotinin, leupeptin and pepstatin (Sigma, St. Louis, MO). The dounced material was filtered through a 70  $\mu\text{m}$  filter (Falcon, Becton-Dickinson, Franklin Lakes, NJ) at 4 °C to yield a "crude cell lysate". The filtration step removes much of the connective tissue. Lamins are so abundant that they were detectable by immunoblotting the crude cell lysate. However, to load enough nuclear equivalents to detect less-abundant nuclear envelope proteins, a "crude nuclear pellet" was prepared by low speed centrifugation (750 g for 10 minutes) at 4 °C followed by re-suspension in TKM buffer. To prepare equivalent fractions from HEP2 hepatocytes, flasks of near confluent HEP2 cells were rinsed twice in PBS, then scraped from the plate into ice-cold TKM buffer containing protease inhibitors. The resulting suspension was dounced as above and centrifuged at 750 g for 10 minutes to prepare a crude nuclear pellet.

To quantify cell numbers for the lamin immunoblotting experiments, an aliquot of the crude cell lysate was mixed with 1% aqueous toluidine blue to count nuclei manually with a hemocytometer. More precise cell counts were obtained in subsequent experiments (LBR, LAP2 and emerin immunoblotting) by assaying an aliquot of material with the DNA-specific dye Hoechst 33258 (Sigma, St Louis, MO). Aliquots of nuclei were first diluted and lysed in TNE buffer (2.0M NaCl, 1 mM EDTA, and 10 mM TRIS-HCl pH 7.4) containing 1.0% sodium dodecyl sulfate (SDS) (Amresco, Solon, OH). We added 10 microliters of the resulting lysate to 2 ml of 0.1  $\mu\text{g/ml}$  Hoechst 33258 in TNE (without SDS) and analyzed with a TKO 100 Fluorometer (Hofer Scientific Instruments, San Francisco, CA). The resulting absorbance was translated to DNA content by interpolating against a plot of DNA standards (calf thymus DNA in 1.0% SDS diluted into TNE buffer as above).

Aliquots of the whole-cell lysate or crude nuclear pellets were mixed with SDS-polyacrylamide gel

## Papillary thyroid carcinoma nuclear envelope

electrophoresis reducing sample loading buffer (final concentration 125 mM Tris, pH 6.8, 4.0% SDS, 2%  $\beta$ -mercaptoethanol, and 20% glycerol), boiled, sonicated to reduce viscosity, and immediately loaded onto 10% polyacrylamide minigels. Pre-labeled molecular weight markers (Gibco BRL Life Technologies, Cat #260 41-020, Gaithersburg, MD) were run in adjacent lanes. Proteins were transferred to nitrocellulose (Micron Separations, Inc, Westborough, MA) by wet blotting according to the manufacturers protocol (Amersham, Arlington Heights, IL). Immunoblotting and chemiluminescent detection was performed with reagents from Amersham according to their protocol. Primary and secondary antibodies were diluted into Tris buffered saline (20 mM Tris, 137 mM NaCl, pH 7.6) with 0.1% Tween-20 and 5% non-fat dry milk. After the primary

antibody, blots were washed extensively (8 times 30 minutes) at room temperature in TRIS buffered saline with 0.1% Tween-20 to reduce background. Under these conditions, the following loadings gave signals near the middle of the curve of signal intensity versus number of nuclei: 5,000-80,000 nuclei for lamin immunoblotting, 100,000-10,000,000 nuclei for emerin and LBR (using HEP2 cells), and 80,000-2,000,000 nuclei for LAP2.

## Results

*Immunofluorescence detection of nuclear envelope proteins in thyroid*

Moderately strong immunostaining intensity was achieved with antibodies against lamin A/C, lamin B1,

Table 1. Cases Studied.

DIAGNOSIS* AND CASE NUMBER	AGE/TNM	PLOIDY	% THYROCYTES	IMMUNOFLUORESCENCE	IMMUNOBLOTTING
PTC-1 (Tall cell variant)	64/T4 NX MX	1.15	49	ND**	Lamins A, B and C; Emerin; LBR
PTC-2	70/T2 N0 MX	1.0	90	ND	Lamins A, B and C; Emerin; LBR
PTC-3	43/T3 NX MX	ND	85	ND	Lamins A, B and C; LBR
PTC-4	60/T1 N0 M0	1.0	79	ND	Lamins A, B and C
PTC-5	74/T4 N0 MX	1.0	94	ND	Lamins A, B, and C; LBR
PTC-6	42/T2 NX MX	1.0	86	ND	Lamins A and C
PTC-7	60/T2 N1b MX	ND	90	Lamins A/C and B	Lamins A and C
PTC-8	58/T2 N1a M0	1.0	93	Lamins A/C and B	Lamin B
PTC-9 (Adjacent to an anaplastic thyroid carcinoma)	85/T4 N1b MX	1.0	ND	Lamins A/C and B; Emerin; 414	ND
PTC-10	33/T2 N1b M0	1.1	ND	Lamins A/C and B; Emerin; LAP 2; 414	Lamins A and C; LAP 2
PTC-11 (Tall cell variant)	50/T4 N1b MX	1.0	85	ND	Lamins A and C; LAP 2
PTC-12	65/T2 N0 MX	1.0	75	ND	Lamins A and C; LAP 2
PTC-13	73/T2 N1a M0	2.1	95	ND	Lamins A and C; LAP 2
PTC-14	44/T2 N1b MX	ND	ND	LAP 2	ND
C-1	27/T2 N0 M0	1.0	89	ND	Lamins A and C; LAP 2
FC-1 (Poorly differentiated, insular type)	66/T2 N1a M1	1.0	94	ND	Lamins A, B, and C
FC-2 (Hurthle cell type)	42/T2 N0 M0	1.0	87	ND	Lamins A, B, and C; Emerin; LBR; LAP 2
FC-3	52/T2 N0 MX	1.0	86	ND	Lamins A, B, and C; Emerin; LBR
FC-4 (Poorly differentiated, insular type)	59/T2 N0 MX	ND	ND	Lamin A/C	ND
FC-5 (Poorly differentiated, insular type)	56/T4 N1a M1	1.0	ND	Lamins A/C and B; Emerin; 414	Lamins A and C; LAP 2
FC-6 (Poorly differentiated)	65/T4 N0 M1	2.77	ND	LAP 2	ND
FA-1	55	1.0	92	ND	Lamins A, B and C
FA-2	75	1.0	79	Lamins A/C and B; Emerin; 414	Lamins A and C; LAP 2
FA-3	47	ND	89	ND	Lamins A and C; LAP 2
NT-1 (From FC-3 patient)	66	ND	85	ND	Lamins A and C; Emerin; LBR
NT-2 (From PTC-4 patient)	74	ND	79	ND	Lamins A and C; LBR
NT-3 (From PTC-7 patient)	60	ND	78	Lamins A/C and B	Lamins A, B and C
NT-4 (Graves disease)	16	ND	83	ND	Lamins A and C, LAP 2

The diagnoses, age and stage ("TNM"), DNA content ("ploidy", where 1 is diploid) and % thyroid cells in the samples are listed. The TNM (Tumor, Node status, Metastasis) stage (Beahrs et al., 1992) corresponds to the time the tissue was procured. Ploidy was determined by flow cytometry on aliquots of the procured tissue, or by image analysis on feulgen stained smears. Percent thyrocytes was measured by manually counting cells in a histologic section adjacent to the procured tissue. Immunofluorescence and immunoblotting were performed with the indicated antibodies. \*: Abbreviations for the diagnoses (Rosai et al., 1992): PTC, papillary thyroid carcinoma; C, well differentiated thyroid carcinoma not otherwise specified; FC, follicular carcinoma; FA, follicular adenoma; NT, non-goiterous, non-inflamed normal thyroid tissue. ND, not done.

emerin, and LAP2. The overall staining intensity with each antibody was comparable for normal thyroid, follicular neoplasms, and PTC samples. The immunostaining patterns for a given specimen were identical whether the cells were fixed with formalin or alcohol. Table 1 lists the diagnoses, TNM characteristics, composition of the tissues, and types of studies performed.

*Immunofluorescence distribution of nuclear envelope proteins in follicular-type epithelium compared to PTC*

As controls for the study of the nuclear envelope in PTC, we first examined normal thyroid cells and follicular neoplasms with relatively spherical nuclei by hematoxylin and eosin staining. Dual staining of a representative formalin-fixed follicular carcinoma (FC-4) with lamin A/C (green) and propidium iodide for chromatin (red) is shown in Fig. 1A-C, in a series of confocal images separated from each other by 1 micron. Note the expected peripheral spherical distribution. Slight cell to cell variation in lamin A/C content is apparent as noted in other tissues (Chaudhary et al., 1990; Cance et al., 1992). Identical immunostaining patterns were seen in smears of normal thyroid cells (data not shown). It is important to note that the confocal microscope collects light in a 0.5  $\mu\text{m}$  thick optical section; when the nuclear envelope is perpendicular to this optical plane, the intensity would be brighter than if the same segment of nuclear envelope were oriented parallel to the optical section. Thus, the fluorescence signal from the pair of cells in the upper right of Fig. 1A is less bright than the same two cells observed in a plane near their equator in Fig. 1C. By directly viewing the cells and focusing through them, the viewer is able to distinguish obliqueness from areas of diminished intensity. In the following images, the best area to judge immunofluorescence intensity is the plane nearest the cell's equator.

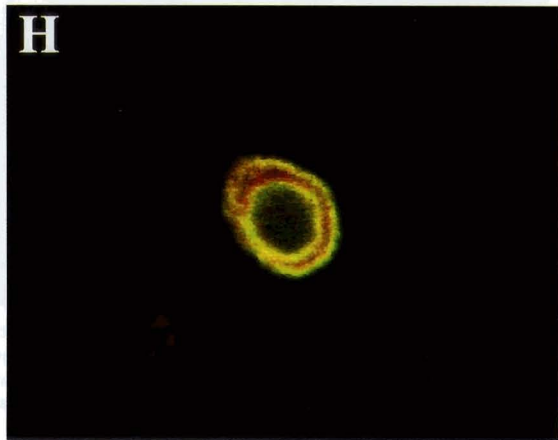
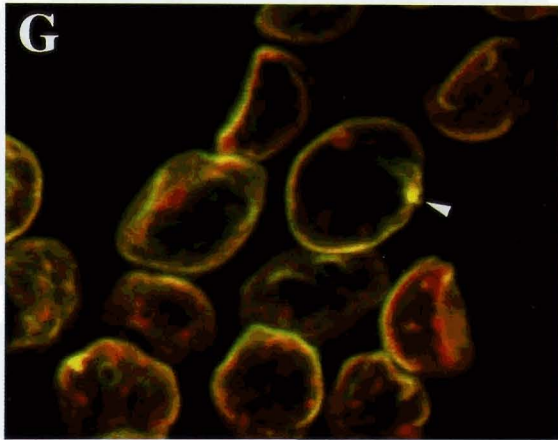
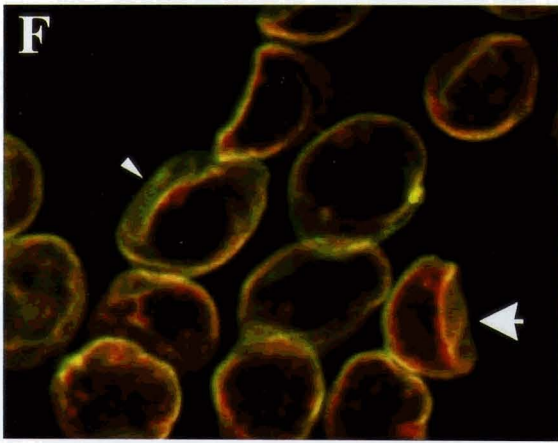
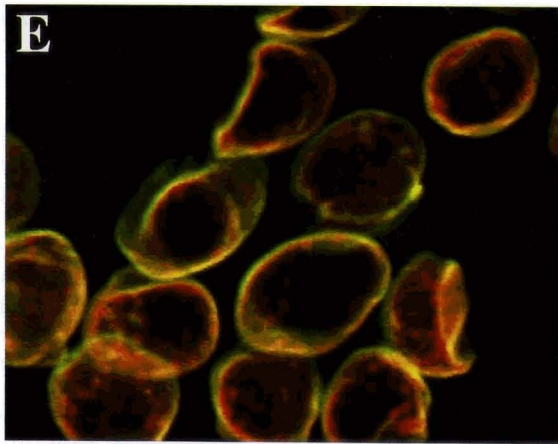
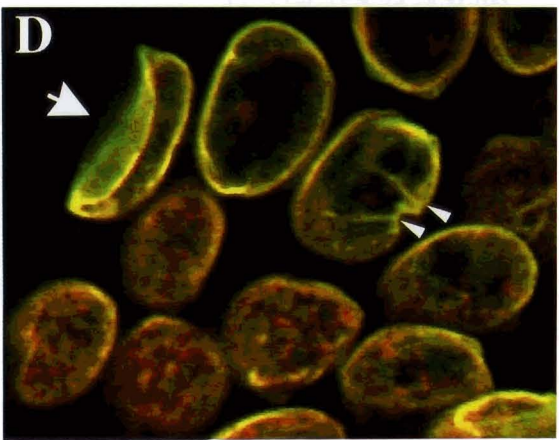
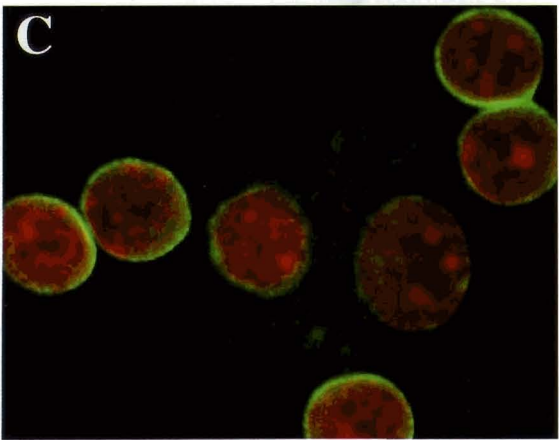
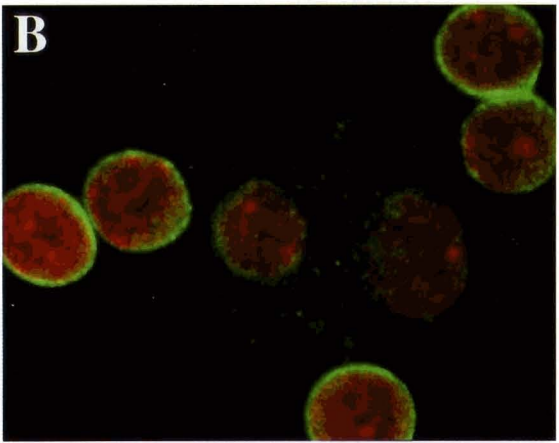
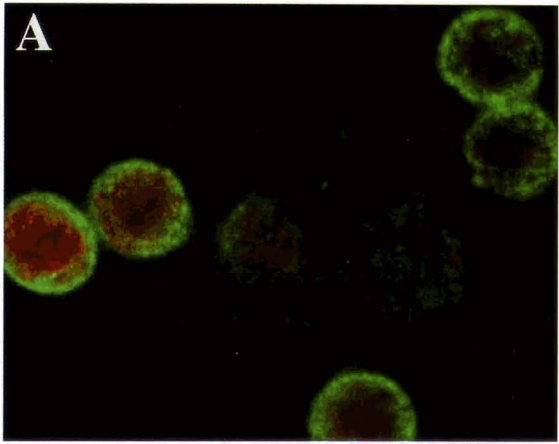
The lamin A/C antibody demonstrates that the nuclear envelope of PTC is highly irregular compared to the follicular samples. For example, Fig. 1D shows

lamin A/C immunostaining (lamins are green, propidium iodide stained DNA is red) in an alcohol fixed PTC (PTC-9). A large intranuclear cytoplasmic inclusion is seen at mid-equatorial level (large arrow). Note that the lamin A/C immunostaining is continuous along the inclusion, with a staining intensity comparable to the opposite, non-deformed side of the nucleus. Another cell shows two lines of increased staining intensity (arrowheads in Fig. 1D) that appear to be shallow creases or folds of the nuclear envelope, too thin to resolve by confocal microscopy. Such lines of lamin immunostaining appear to correspond to very thin nuclear grooves in corresponding hematoxylin and eosin stained smears. A variation in staining intensity of PTC samples from cell to cell is observed with the lamin A/C antibody (Fig. 1D) similar to the variation in the follicular samples.

Lamin B1 immunostaining is more uniform in intensity from cell to cell in both follicular-type epithelium and PTC. Otherwise, its staining pattern is similar to that of lamin A/C. Fig. 1E-G shows the distribution of lamin B1 in an alcohol-fixed PTC (PTC-9) in a series of confocal images separated by 1  $\mu\text{m}$ . The fluorescence intensity is continuous along an intranuclear inclusion (large arrow in Fig. 1F) and throughout the full contour of a nuclear groove (cell marked with an arrowhead in Fig. 1F). The staining intensity in the grooves and inclusions is comparable to the non-deformed side of the nucleus.

Occasional foci of increased staining for nuclear envelope proteins are sometimes observed along the nuclear periphery in PTC. For example, the cell marked with an arrowhead in Fig. 1G has a bright focus that is also visible in adjoining sections (Fig. 1E,F). These foci of bright staining do not correlate with the locations of contour irregularity, including grooves or inclusions. Dual immunostaining (see below) for lamins, emerin, or nuclear pore complexes shows that these bright foci stain strongly for multiple antigens. We suspect that these bright foci represent highly folded zones in the nuclear envelope, rather than an area of increased thickness of the lamina itself.

**Fig. 1.** Confocal imaging of lamin A/C, lamin B1, and emerin in thyroid neoplasms. For all images, red is the propidium iodide staining of chromatin, and green/yellow is the FITC label for nuclear envelope proteins. Final magnification is 2000, covering a field of about 37  $\mu\text{m}$  in length. Each confocal optical section is 0.5  $\mu\text{m}$  in thickness. **A-C** show the distribution of lamin A/C in a series of confocal images separated from each other by 1  $\mu\text{m}$  in a formalin fixed smear of a follicular carcinoma (case FC-4). Note the slight variability from cell to cell in staining intensity, and the round nuclear envelope contour. **D** shows the lamin A/C distribution in a smear of an alcohol fixed PTC (case PTC-9). Note the continuous distribution of lamin A/C across the large intranuclear cytoplasmic inclusion (arrow). The staining intensity of lamin A/C in the region of the intranuclear cytoplasmic inclusion is the same as the opposite (or convex) surface of the same cell's nuclear envelope. One cell has two thin apparent creases (arrowheads) in the nuclear envelope (see text). There is some variability in the lamin A/C staining intensity from cell to cell in Fig. 1D, similar to the variability in the follicular carcinoma sample in Figs. 1A-C. **E-G** show the lamin B1 distribution in the same alcohol fixed PTC case as in Fig. 1D (case PTC-9). At least two intranuclear cytoplasmic inclusions and several grooved cells are present and are displayed in sequential confocal images separated from each other by 1  $\mu\text{m}$ . The intranuclear cytoplasmic inclusion marked with an arrow in Fig. 1F can be seen to be lined continuously with lamin B1 at the same relative intensity as the convex surface of the same nucleus. Continuous lamin B staining is also seen throughout the depths of a nuclear groove (cell marked with an arrowhead in Fig. 1F) and the intensity of immunostaining in this groove is the same as the more rounded parts of the same cell's nuclear envelope. Occasional foci of bright staining are seen, for example the cell marked with an arrow head in Fig. 1G. These bright foci may represent highly folded areas of the nuclear envelope and do not bear any consistent relation to the presence or location of nuclear grooves or inclusions. **H** shows emerin continuously lining the outer perimeter and entirely lining the surface of a large intranuclear inclusion in a single PTC cell (PTC-9) from a formalin fixed smear. The staining intensity in the inclusion is the same as the rest of the nuclear envelope. x 2,000



*Papillary thyroid carcinoma nuclear envelope*

In a given thyroid sample, the immunostaining pattern of emerin is indistinguishable from that of lamin B1. Emerin staining is continuous along all parts of the nuclear envelope in both PTC and normal thyroid. Emerin staining is continuous along a large intranuclear cytoplasmic inclusion in Fig. 1H, with an intensity equal to the rest of the nuclear envelope. A follicular adenoma (FA-2) with the typical spherical nuclear shape also shows continuous staining along the nuclear envelope when immunostained with emerin (Fig. 2B).

A LAP2 polyclonal antibody raised against amino acids 1-187 of human LAP2 showed strong immunoreactivity at the nuclear envelopes of both follicular and PTC cells. The LAP2 immunostaining pattern is indistinguishable from that of lamin B1 or emerin. LAP2 immunofluorescent staining of a formalin fixed PTC (PTC-14) is shown in Fig. 2A. Again, continuous staining of the nuclear periphery, and continuous staining of an intranuclear cytoplasmic inclusion (arrowhead) are seen. The intensity of LAP2 immuno-

staining is the same in the relatively spherical parts of the nuclear envelope as it is in grooves and inclusions.

Antibody 414, recognizing an epitope common to a number of nuclear pore proteins, gave a finely punctate staining pattern along the nuclear envelope of both PTC (PTC-14, Fig. 2C) and follicular epithelium (FA-2, a follicular adenoma, Fig. 2D). Nuclear pore complexes are not excluded from either the intranuclear cytoplasmic inclusions or grooves of PTC nuclei.

We considered the possibility that a subset of the nuclear envelope irregularities in PTC might lack nuclear envelope structural protein(s), and therefore would be difficult to detect. This appears unlikely for the following reasons: First, nuclear envelope irregularities are independently revealed by the propidium iodide counterstain. In all PTC samples, the distribution of nuclear envelope proteins was continuous with the propidium iodide-stained outer edge of chromatin. Second, dual immunostaining for lamins A/C or B1, with either emerin or nuclear pore complexes showed

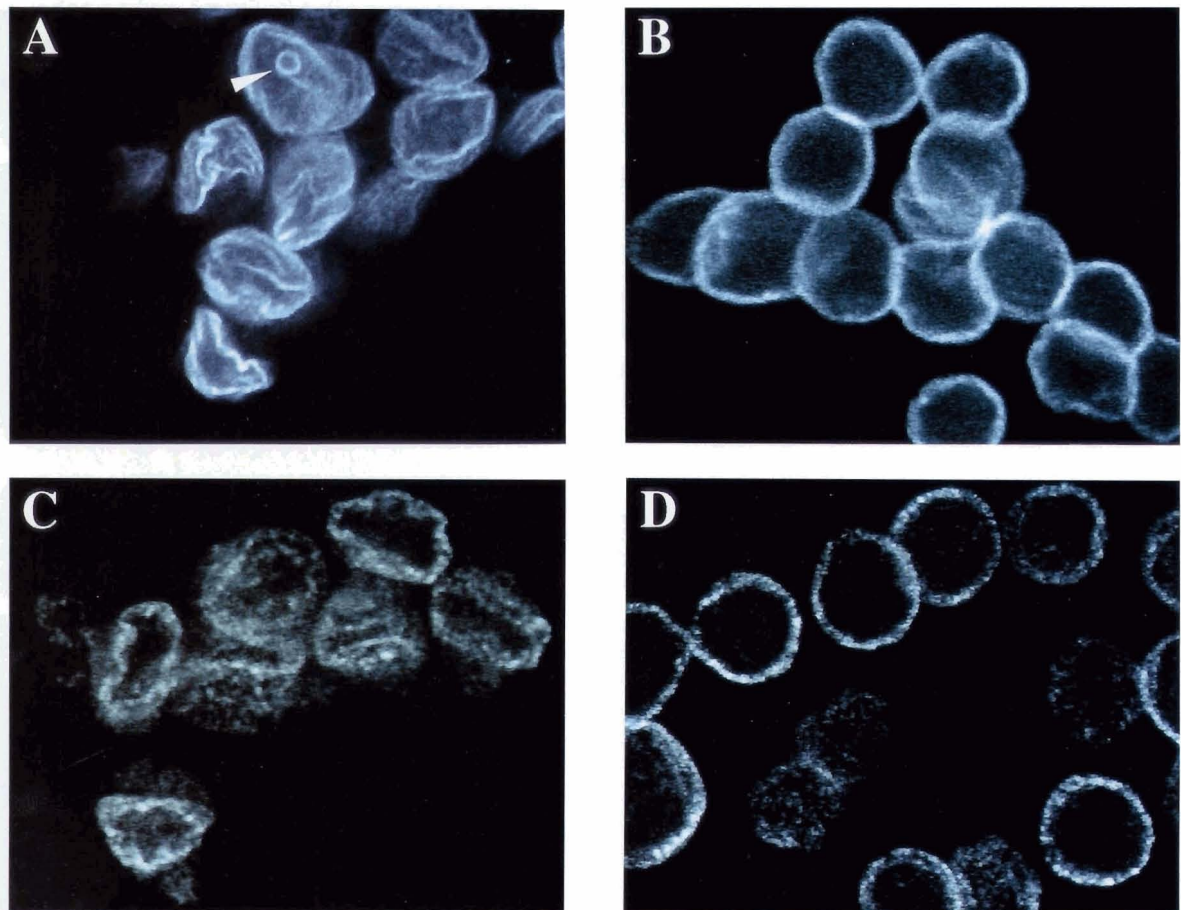


**Fig. 2.** Confocal imaging of LAP 2, emerin, and nuclear pores in thyroid neoplasms. **A** shows a formalin fixed PTC sample (case PTC-10) stained with an antibody raised against an epitope shared by all known LAP2 isoforms. Note the continuous, even staining pattern around the highly irregular nuclear contour, and the staining of a small intranuclear cytoplasmic inclusion (arrowhead). **B** shows the emerin immunostaining pattern in a formalin fixed follicular adenoma (FA-2). **C and D** show the nuclear pore distribution in formalin fixed PTC cells and follicular adenomas (cases PTC-10 and FA-2, respectively). Nuclear pores can be seen to follow the entire irregular nuclear contour of PTC. x 2,000

## Papillary thyroid carcinoma nuclear envelope

that nuclear envelope proteins always colocalized in PTC (not shown). This analysis would have disclosed domains of the nuclear envelope devoid of one nuclear envelope protein. Finally, the degree and quality of the nuclear irregularity in hematoxylin and eosin stained smears of these PTC samples was comparable to the immunostained appearance of the nuclear envelope.

### *Electrophoretic mobility and relative abundance of lamins A, C and B1*

Immunoblotting showed that the electrophoretic mobilities of lamins A, C, and B1 are the same in PTC and follicular thyroid samples (Figs. 3A,B). The calculated molecular weights are approximately 72 kD for lamin A, 62 kD for lamin C, and 67 kD for lamin B. By loading known numbers of nuclei (see Methods), we estimated the relative amounts of each lamin per cell. For each sample, three different numbers of nuclei were run, and for a given comparison, all samples were blotted, probed, and developed together. Lamins A, C and B1 all become detectable at 5,000 to 20,000 nuclei per lane (Figs. 3A,B). In the series shown, PTC tends to have more lamin A/C than normal thyroid or follicular adenomas, a finding *opposite* to predictions in the literature that lamin A/C content should be lower in proliferating cells (Chaudhary et al., 1990; Cance et al., 1992; reviewed in Bosman, 1996; Coates et al., 1996). In other experiments, some follicular neoplasms had more lamin A/C than the PTC samples to which they were compared (not shown). Overall, there was no correlation between lamin A/C content and clinical or pathological features.

We noted that the ratio of lamin A and C band intensities was not always equal. For example lamin A appeared slightly less abundant than lamin C in PTC-6 (Fig. 3A). In addition, some faint lower molecular weight bands are seen in PTC-6 and PTC-7. These may represent degradation, since this pattern could be reproduced by processing the thawed tissue at room temperature rather than on ice (not shown). The altered ratio of lamin A to C was also sometimes observed in follicular samples. A low ratio of lamin A to C has been observed in other tissues, including erythroid precursor cells (Martelli et al., 1992), and embryonal carcinoma of the testis (Machiels et al., 1997).

### *Electrophoretic mobility and relative amount of emerin*

The electrophoretic mobility of emerin is identical for all samples studied (Fig. 3C), and is calculated to be 34 kD. There is no consistent difference in the relative amount of emerin between PTC and follicular samples.

### *Sparse or absent LBR in the thyroid*

An affinity-purified antibody against human LBR detected a single band of the appropriate size (~58 kD) in HEP2 cells, a human hepatocyte cell line (Fig. 3D).

This band was detectable when loading as few as 100,000 nuclei. In contrast, LBR was not detected when loading 10,000,000 nuclei from thyroid samples, with one exception: case PTC-1, which contains a high proportion of non-thyroid cells, displayed a distinct single 58 kD band at high nuclear loadings in longer exposures (not shown). The same nuclear preparations contain an appropriate amount of non-degraded lamins by immunoblotting (data not shown), demonstrating that the quantification of nuclei was correct and that the samples were not proteolytically degraded. We conclude that immunoreactive LBR, if it is present at all in thyroid cells, is expressed at less than 1% of the level in HEP2 hepatocytes per cell. Since some of our samples contained a significant proportion of admixed lymphocytes, plasma cells, and stromal cells (see Table 1), the abundance of LBR also appears to be low in these non-thyroid cells, compared to HEP2 cells.

### *LAP2 isoforms in the thyroid*

The LAP2 antibody specifically recognized three major bands of approximately 76, 54 and 38 kD in HEP2 cells and thyroid samples. Five representative thyroid samples probed with LAP2 antibody are shown in Fig. 3E. The three principal bands correspond closely to the expected masses of the known LAP2 isoforms - $\alpha$ , - $\beta$ , and - $\gamma$ . Two other minor bands of about 50 and 40 kD were also seen in some samples. No bands were detected with pre-immune serum from rabbit #2804 (not shown). There is some variation in the relative intensities of the bands, but with no correlation to clinicopathologic features. The 76 kD band is not evident in sample PTC-12 at the exposure shown, but is evident with longer exposure (not shown). Of two follicular adenomas studied, one (FA-3) had a relatively weak 38 kD band (Fig. 3E), and the other (FA-2) had a relatively strong 38 kD band (not shown).

### *Attempts to purify PTC nuclei in sucrose gradients*

As a first step in producing purified PTC nuclear envelopes, we attempted to purify nuclei using high speed sedimentation of crude nuclear pellets in 2.3M sucrose, according to a standard protocol for isolating pure hepatocyte nuclei (Dwyer and Blobel, 1976). Purified thyroid cell nuclei were isolated from crude nuclear pellets with yields >40% in four of four attempts from normal thyroid and follicular neoplasms, but the yield of purified nuclei from PTC samples was very low in two of three attempts (data not shown). This may be due to a buoyancy of the PTC nuclei. Repeat sedimentation of fewer cells in 1.8M sucrose solutions did not improve percent yield. Variation in the "buoyancy" of nuclei of different cell types has been previously observed (Pederson and Spann, 1998). The PTC nuclei that sedimented were morphologically indistinguishable from the nuclei of non-sedimenting PTC cases. Interestingly, sucrose-purified unfixed nuclei

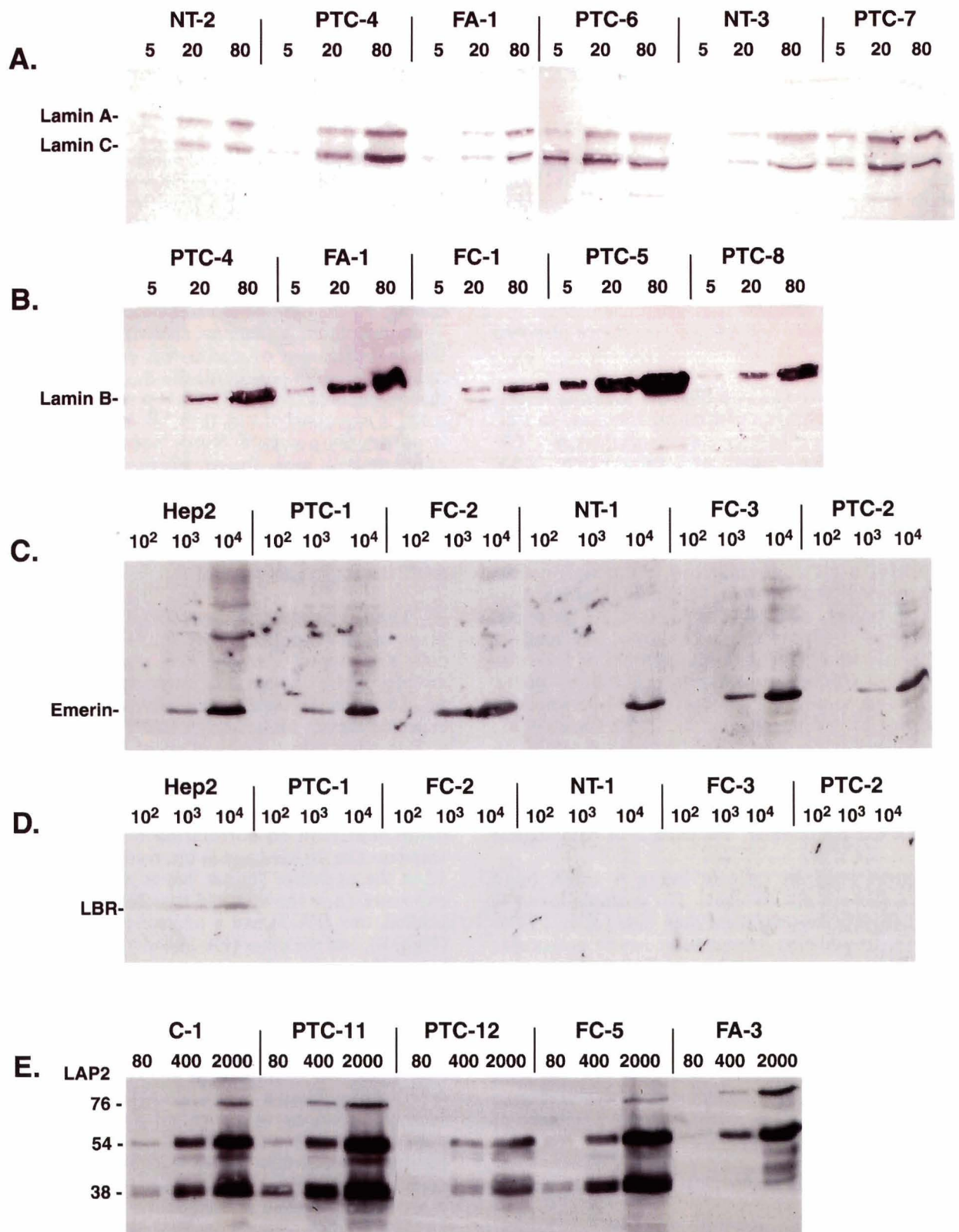


**Fig. 3.** Immunoblotting of lamins, emerlin, lamin B receptor and LAP2 proteins. Representative results of a survey of nuclear envelope proteins is shown. For a given antibody, known numbers of nuclei (shown above each lane  $\times 10^{-3}$ ) were loaded, electrophoresed, immunoblotted, and exposed together to allow comparison of the relative amounts on a per cell basis. The molecular weights were measured against pre-stained molecular weight standards loaded onto the same gels. The calculated molecular weights, in accordance with previous reports, are 72 and 62 kD for lamins A and C (**A**), 67 kD for lamin B (**B**), 34 kD for emerlin (**C**), 58 kD for lamin B receptor (**D**), and 76, 54 and 38 kD for the  $\alpha$ ,  $\beta$  and  $\gamma$  isoforms of LAP2 (**E**). For lamin B receptor, a very faint band at the expected molecular weight of 58 kD is apparent when loading 100,000 HEP2 (human hepatocyte) nuclei, whereas no bands are apparent when loading up to 10,000,000 nuclei of any of the thyroid samples at the exposure shown. For each of the other antibodies, the relative amounts and electrophoretic mobilities overlap between PTC and follicular samples. The LAP2 $\alpha$  band is not evident in the PTC-12 sample at the exposure shown, but is apparent at longer exposures. Possible minor isoforms of LAP2 proteins are also seen in all the samples shown in this Fig. (see text).

from frozen tissue, stripped of cytoplasm, retain the distinctive nuclear contour features of either follicular neoplasms or PTC.

## Discussion

Our study suggests that the irregular nuclear contour of papillary thyroid carcinoma is not due to alterations in the expression or localization of lamins, emerin, LAP2 or LBR. Specifically, intranuclear cytoplasmic inclusions or grooves do not result from a localized deficiency of any of the structural envelope proteins studied, nor is there any obvious alteration in the distribution of lamins, LAP2, emerin, or nuclear pore complexes with respect to the nuclear contour alterations in PTC. The distribution of these major nuclear envelope proteins appears simply to conform to the contour of the irregular nucleus in PTC. The relative abundance and electrophoretic mobility of the nuclear lamina proteins did not differ between PTC and follicular-type epithelium. These results are surprising since the nuclear lamina appears to play a central role in defining nuclear shape. For example, expression of mutant lamins, or altered expression of lamins or LAP2 affects nuclear contour (Loewinger and McKeon, 1988; Furukawa and Hotta, 1993; Ellis et al., 1997; Lenz-Bohme et al., 1997). Very recent studies in *C.elegans* confirms a role for lamins in defining nuclear shape: timelapse video imaging demonstrates that the contour of lamin-deficient nuclei of *C. elegans* changes significantly and rapidly, every 30 seconds, in living embryonic cells (Y. Gruenbaum, personal communication). Lamins may therefore be required for nuclei to resist deforming forces that arise continuously either from inside or outside the nucleus. We did not study lamin B2 or LAP1, and our analysis cannot exclude subtle electrophoretic mobility changes in the six proteins that were studied. Nevertheless, in the absence of detectable changes in the expression of six principle nuclear envelope proteins, we think it reasonable to consider alternative hypotheses for the changes in nuclear shape of PTC cells: nuclear contour may be controlled by a balance between forces exerted on the nuclear envelope from the inside (by chromatin or the nuclear matrix) and the outside (cytoskeleton). We hypothesize that this balance is disturbed in PTC cells. We speculate this balance may be actively regulated in certain cell types, such as white blood cell precursors, in which the shape of the nucleus changes dramatically during differentiation.

Chromatin and nuclear matrix proteins may directly influence nuclear contour, for two reasons. First, PTC nuclei stripped of cytoplasm appear to retain their shape irregularities. Second, RET/PTC is known to affect chromatin as well as the nuclear envelope (Fischer et al., 1998a) and PTC itself shows both chromatin as well as nuclear envelope changes. If chromatin effects a change in the shape of the nuclear envelope, it is not apparently due to gross changes in the chromatin-associated proteins LBR, LAP2, or emerin. The nuclear matrix is

the complex biochemical fraction that remains after extraction with deoxyribonuclease, non-ionic detergent and salt. Electron microscopy of resinless sections of the nuclear matrix displays filaments that physically contact the nuclear lamina (reviewed by Nickerson, 1998). The nature of these nuclear matrix filaments is not well understood. They may include lamins themselves, since some lamins have been found within the nuclear interior in many organisms (Moir et al., 1995; Paddy et al., 1996; Y. Gruenbaum, personal communication). Another chromatin-associated protein that may influence nuclear contour is actin, which has been unequivocally localized in the nucleus (reviewed by Rando et al., 2000). Nuclear actin may have a predominantly peripheral distribution (Clubb and Locke, 1998), perhaps as a consequence of binding to lamin A (Sasseville and Langelier, 1998).

The cytoskeleton can influence nuclear contour. For example cell lines that lack cytoplasmic intermediate filaments have more irregular nuclear contours than the same cell lines in which intermediate filament expression has been restored, suggesting that the cytoskeleton is able to constrain nuclear contour (Sarria et al., 1994) (however, see conflicting results of Holwell et al., 1997). Expression of mutant keratins causes abnormalities in nuclear shape (Fuchs et al., 1992). Furthermore, bundles of cytoplasmic intermediate filaments have been observed within nuclear folds in a pancreatic adenocarcinoma cell line, and have appeared to physically indent the nucleus (Kamei, 1994). Direct micromanipulation of integrins at the plasma membrane deforms the nucleus, and even causes movement of nucleoli (Maniotis et al., 1997). Nuclei are frequently indented next to the centrosome (e.g. Shu and Joshi, 1995), as if the microtubule system that they organize pushes on the nuclear envelope. Resinless section electron microscopy has demonstrated cytoplasmic filaments that appear to directly attach to the nuclear lamina (reviewed in Nickerson, 1998). However, the molecular basis for interactions of the cytoskeleton with the nuclear envelope remains obscure (Goldman et al., 1985; Georgatos and Blobel, 1987; Albers and Fuchs, 1989).

### *Potential functional significance of altered nuclear envelope contour in cancer*

The fact that nuclear contour changes are so common in cancer cells, often from an early stage in cancer development, and that they appear conserved during the subsequent evolution of cancer cells should indicate that alterations in nuclear contour are functionally significant. Several nuclear envelope proteins appear to affect replication competence, including lamins A/C, B, and LAP2. B-type lamins are strongly implicated in positively regulating DNA replication, as demonstrated in "artificial" nuclei. "Artificial" nuclei can be assembled around sperm chromatin using nuclear envelope-derived vesicles from meiotic *Xenopus* egg extracts. When lamin B is

immunodepleted from these egg extracts, the nuclei are unable to replicate (Newport et al., 1990; Jenkins et al., 1993). Replication competence in this model is specifically restored by re-addition of lamin B (Goldberg et al., 1995). The mechanism by which lamin B may influence replication competence is unknown. Of possible relevance is the finding that a fraction of B type lamins are present in intranuclear foci that colocalize during S-phase with sites of replication (Moir et al., 1994). Dominant disrupting mutant lamin proteins—which disturb the normal peripheral rim distribution of lamin B—also diminish or prevent replication (Ellis et al., 1997; Spann et al., 1997). Supporting the hypothesis that lamin B is important in determining replication competence is the observation that its expression tends to be higher in stem cells (Broers et al., 1997; Machiels et al., 1997) compared to terminally differentiated cells.

In contrast to B-type lamins, the expression of lamins A and C is implicated in loss of replication competence and terminal differentiation (reviewed in Moir et al., 1995; Bosman, 1996). For example, crypt cells of the intestines and basal keratinocytes do not express lamin A/C, whereas cells higher in the crypts or epidermis do express lamins A/C (Chaudhary et al., 1990; Cance et al., 1992; Coates et al., 1996). Lamins A/C can interact with the retinoblastoma (Rb) gene product *in vitro*, and they partly colocalize with Rb *in vivo*, leading to speculation that lamins A/C may influence Rb function (Mancini et al., 1994).

LAP2 may also regulate DNA replication competence: when "artificial" assembling nuclei are exposed to exogenous LAP2 $\beta$  polypeptides, either *in vitro* or by microinjection into post-mitotic cells, nuclear growth is inhibited (Yang et al., 1997; Gant et al., 1999). When added to assembling nuclei in *Xenopus* extracts at low micromolar concentrations, LAP2 $\beta$  can increase the efficiency of DNA replication (Gant et al., 1999); however replication is inhibited by higher concentrations of LAP2 $\beta$  (Yang et al., 1997; Gant et al., 1999). A study of LAP2 expression in adult rat tissues showed tissue-specific expression of LAP2 isoforms, with some tendency for higher LAP2 $\beta$  expression in tissues with high proliferative activity (Ishijima et al., 1996).

We found no relation between the relative amounts of lamin A/C, B1 or LAP2 proteins and clinico-pathological features predictive of replication rate in the thyroid. In fact, the average amount of lamin A/C per cell appears sometimes *higher* for follicular neoplasms or PTC than normal non-neoplastic thyroid (Fig. 3A). An immunohistochemical study also showed that normal, regenerating, and neoplastic hepatocytes all express lamin A/C (Hytiroglou et al., 1993). Although the amounts of these nuclear lamina proteins appear unaltered, the increased nuclear envelope surface area of PTC might influence replication competence, through more extensive contacts between the envelope and chromatin. Furthermore, since there was cell-to-cell variability in lamin A/C staining intensity in our samples (e.g. Figs. 1A-D), we cannot exclude the possibility that

replication competence is retained selectively in neoplastic thyroid cells with diminished lamin A/C content.

LBR had been thought to be widely expressed, but we found that LBR, if it is expressed at all in the thyroid, is present at less than 1% the level of hepatocytes. The absence or paucity of LBR in the thyroid suggests that its proposed roles in targeting postmitotic nuclear envelope vesicles to chromatin (Pyrpasopoulou et al., 1996), or organizing heterochromatin at the nuclear envelope (Ye et al., 1998) can be performed by other proteins.

#### *The thyroid as a model for studying large scale nuclear organization*

The study sample in Table 1 demonstrates the usefulness of the thyroid as a model for studying the molecular basis of diagnostic structural changes in cancer cells. Normal and tumorous crude thyroid samples are relatively homogeneous, typically with about 85% tumor cells and only rare mitotic figures. Most thyroid tumors are diploid, alleviating the problems of genetic instability and tumor cell heterogeneity that plague studies of other common solid tumors. Since their histogenesis is the same, the molecular features of PTC and follicular neoplasms can be readily compared. The two pathways that transform normal thyroid epithelial cells are genetically distinct, and the morphologic features associated with these two pathways can be reproduced in an *in vitro* model system (Bond et al., 1994; Fischer et al., 1998a).

---

*Acknowledgments.* Supported by a grant from the W.W. Smith Charitable Trust (H9702) to K.L.W.

---

#### References

- Albers K. and Fuchs E. (1989). Expression of mutant keratin cDNAs in epithelial cells reveals possible mechanisms for initiation and assembly of intermediate filaments. *J. Cell Biol.* 108, 1477-1493.
- Beahrs O.H., Henson D.E., Hutter R.V.P. and Kennedy B.J. (1992). American Joint Committee on Cancer: Manual for Staging of Cancer. 4th edition. J. B. Lippincott. Philadelphia.
- Berger R., Theodor L., Shoham J., Gokkel E., Brok-Simoni F., Avraham K.B., Copeland N.G., Jenkins N.A., Rechavi G. and Simon A.J. (1996). The characterization and localization of the mouse thymopoietin/lamina-associated polypeptide 2 gene and its alternatively spliced products. *Genome Res.* 6, 361-370.
- Bond J.A., Wyllie F.S., Rowson J., Radulescu A. and Wynford-Thomas D. (1994). *In vitro* reconstruction of tumour initiation in a human epithelium. *Oncogene* 9, 281-290.
- Bonne G., Di Barletta M.R., Varnous S., Becane H.M., Hammouda E.H., Merlini L., Muntoni F., Greenberg C.R., Gary F., Urtizberea J.A., Duboc D., Fardeau M., Toniolo D. and Schwartz K. (1999). Mutations in the gene encoding lamin A/C cause autosomal dominant Emery-Dreifuss muscular dystrophy. *Nat. Genet.* 21, 285-288.

*Papillary thyroid carcinoma nuclear envelope*

- Bosman F.T. (1996). Nuclear structure and the lamins. *J. Pathol.* 178, 3-4.
- Broers J.L., Machiels B.M., Kuijpers H.J., Smedts F., van den Kieboom R., Raymond Y. and Ramaekers F.C. (1997). A- and B-type lamins are differentially expressed in normal human tissues. *Histochem. Cell Biol.* 107, 505-517.
- Cance W.G., Chaudhary N., Worman H.J., Blobel G. and Cordon-Cardo C. (1992). Expression of the nuclear lamins in normal and neoplastic human tissues. *J. Exp. Clin. Cancer Res.* 11, 233-246.
- Chaudhary N. and Courvalin J.C. (1993). Stepwise reassembly of the nuclear envelope at the end of mitosis. *J. Cell Biol.* 122, 295-306.
- Chaudhary N., Chance W.G., Worman H.J., Blobel G. and Cordon-Cardo C. (1990). Nuclear lamin expression in normal and neoplastic human tissues. *J. Cell Biol.* 111, 375a.
- Clubb B.H. and Locke M. (1998). Peripheral nuclear matrix actin forms perinuclear shells. *J. Cell Biochem.* 70, 240-251.
- Coates P.J., Hobbs R.C., Crocker J., Rowlands D.C., Murray P., Quinlan R. and Hall P.A. (1996). Identification of the antigen recognized by the monoclonal antibody BU31 as lamins A and C. *J. Pathol.* 178, 21-29.
- Dechat T., Gotzmann J., Stockinger A., Harris C.A., Talle M.A., Siekierka J.J. and Foisner R. (1998). Detergent-salt resistance of LAP2 in interphase nuclei and phosphorylation-dependent association with chromosomes early in nuclear assembly implies functions in nuclear structure dynamics. *EMBO J.* 17, 4887-4902.
- Dwyer N. and Blobel G. (1976). A modified procedure for the isolation of a pore complex-lamina fraction from rat liver nuclei. *J. Cell Biol.* 70, 581-591.
- Ellis D.J., Jenkins H., Whitfield W.G. and Hutchison C.J. (1997). GST-lamin fusion proteins act as dominant negative mutants in *Xenopus* egg extract and reveal the function of the lamina in DNA replication. *J. Cell Sci.* 110, 2507-2518.
- Emery A.E. (1989). Emery-Dreifuss syndrome. *J. Med. Genet.* 26, 637-641.
- Fischer A.H., Bond J.A., Taysavang P., Battles O.E. and Wynford-Thomas D. (1998a). Papillary thyroid carcinoma oncogene (RET/PTC) alters the nuclear envelope and chromatin structure. *Am. J. Pathol.* 153, 1443-1450.
- Fischer A.H., Chadde D.N., Wright J.A., Gansler T.S. and Davie J.R. (1998b). Ras-associated nuclear structural change appears functionally significant and independent of the mitotic signaling pathway. *J. Cell Biochem.* 70, 130-140.
- Foisner R. and Gerace L. (1993). Integral membrane proteins of the nuclear envelope interact with lamins and chromosomes, and binding is modulated by mitotic phosphorylation. *Cell* 73, 1267-1279.
- Frost J.K. (1986). *The cell in health and disease: An evaluation of cellular morphologic expression of biologic behavior.* Karger, New York.
- Fuchs E., Esteves R.A. and Coulombe P.A. (1992). Transgenic mice expressing a mutant keratin 10 gene reveal the likely genetic basis for epidermolytic hyperkeratosis. *Proc. Natl. Acad. Sci. USA* 89, 6906-6910.
- Furukawa K. (1999). LAP2 binding protein 1 (L2BP1/BAF) is a candidate mediator of LAP2-chromatin interaction. *J. Cell Sci.* 112, 2485-2492.
- Furukawa K. and Hotta Y. (1993). cDNA cloning of a germ cell specific lamin B3 from mouse spermatocytes and analysis of its function by ectopic expression in somatic cells. *EMBO J.* 12, 97-106.
- Gant T.M. and Wilson K.L. (1997). Nuclear assembly. *Annu. Rev. Cell Dev. Biol.* 13, 669-695.
- Gant T.M., Harris C.A. and Wilson K.L. (1999). Roles of LAP2 proteins in nuclear assembly and DNA replication: Truncated LAP2B proteins alter lamina assembly, envelope formation, nuclear size, and DNA replication efficiency in *Xenopus laevis* extracts. *J. Cell Biol.* 144, 1083-1096.
- Georgatos S.D. and Blobel G. (1987). Two distinct attachment sites for vimentin along the plasma membrane and the nuclear envelope in avian erythrocytes: a basis for a vectorial assembly of intermediate filaments. *J. Cell Biol.* 105, 105-115.
- Georgatos S.D., Meier J. and Simos G. (1994). Lamins and lamin-associated proteins. *Curr. Opin. Cell Biol.* 6, 347-353.
- Gerace L. and Foisner R. (1994). Integral membrane proteins and dynamic organization of the nuclear envelope. *Trends Cell Biol.* 4, 127-131.
- Goldberg M., Jenkins H., Allen T., Whitfield W.G. and Hutchison C.J. (1995). *Xenopus* lamin B3 has a direct role in the assembly of a replication competent nucleus: evidence from cell-free egg extracts. *J. Cell Sci.* 108, 3451-3461.
- Goldman R., Goldman A., Green K., Jones J., Lieska N. and Yang H.Y. (1985). Intermediate filaments: possible functions as cytoskeletal connecting links between the nucleus and the cell surface. *Ann. NY Acad. Sci.* 455, 1-17.
- Harris C.A., Andryuk P.J., Cline S.W., Mathew S., Siekierka J.J. and Goldstein G. (1995). Structure and mapping of the human thymopoietin (TMPO) gene and relationship of human TMPO beta to rat lamin-associated polypeptide 2. *Genomics* 28, 198-205.
- Heidemann S.R., Kaeck S., Buxbaum R.E. and Matus A. (1999). Direct observations of the mechanical behaviors of the cytoskeleton in living fibroblasts. *J. Cell Biol.* 145, 109-122.
- Holwell T.A., Schweitzer S.C. and Evans R.M. (1997). Tetracycline regulated expression of vimentin in fibroblasts derived from vimentin null mice. *J. Cell Sci.* 110, 1947-1956.
- Hytiroglou P., Choi S.W., Theise N.D., Chaudhary N., Worman H.J. and Thung S.N. (1993). The expression of nuclear lamins in human liver: an immunohistochemical study. *Hum. Pathol.* 24, 169-172.
- Ishijima Y., Toda T., Matsushita H., Yoshida M. and Kimura N. (1996). Expression of thymopoietin beta/lamina-associated polypeptide 2 (TP beta/LAP2) and its family proteins as revealed by specific antibody induced against recombinant human thymopoietin. *Biochem. Biophys. Res. Commun.* 226, 431-438.
- Jenkins H., Holman T., Lyon C., Lane B., Stick R. and Hutchison C. (1993). Nuclei that lack a lamina accumulate karyophilic proteins and assemble a nuclear matrix. *J. Cell Sci.* 106, 275-285.
- Johannessen J.V., Sobrinho-Simoes M., Finseth I. and Pilstrom L. (1982). Papillary carcinomas of the thyroid have pore-deficient nuclei. *Int. J. Cancer* 30, 409-411.
- Johannessen J.V., Sobrinho-Simoes M., Finseth I. and Pilstrom L. (1983). Ultrastructural morphometry of thyroid neoplasms. *Am. J. Clin. Pathol.* 79, 166-171.
- Kamei H. (1994). Relationship of nuclear invaginations to perinuclear rings composed of intermediate filaments in MIA PaCa-2 and some other cells. *Cell Struct. Funct.* 19, 123-132.
- Klugbauer S., Demidchik E.P., Lengfelder E. and Rabes H.M. (1998). Detection of a novel type of RET rearrangement (PTC5) in thyroid carcinomas after Chernobyl and analysis of the involved RET-fused gene RFG5. *Cancer Res.* 58, 198-203.
- Lanoix J., Skup D., Collard J.F. and Raymond Y. (1992). Regulation of the expression of lamins A and C is post-transcriptional in P19

*Papillary thyroid carcinoma nuclear envelope*

- embryonal carcinoma cells. *Biochem. Biophys. Res. Commun.* 189, 1639-1644.
- Lee M.S. and Craigie R. (1998). A previously unidentified host protein protects retroviral DNA from autointegration. *Proc. Nat. Acad. Sci. USA* 95, 1528-1533.
- Lemoine N.R., Mayall E.S., Wyllie F.S., Williams E.D., Goyns M., Stringer B. and Wynford-Thomas D. (1989). High frequency of ras oncogene activation in all stages of human thyroid tumorigenesis. *Oncogene* 4, 159-164.
- Lenz-Bohme B., Wismar J., Fuchs S., Reifegerste R., Buchner E., Betz H. and Schmitt B. (1997). Insertional mutation of the *Drosophila* nuclear lamin Dm0 gene results in defective nuclear envelopes, clustering of nuclear pore complexes, and accumulation of annulate lamellae. *J. Cell Biol.* 137, 1001-1016.
- LiVolsi V.A. (1990). *Surgical pathology of the thyroid*. W.B. Saunders, Philadelphia, PA.
- Loewinger L. and McKeon F. (1988). Mutations in the nuclear lamin proteins resulting in their aberrant assembly in the cytoplasm. *EMBO J.* 7, 2301-2309.
- Machiels B.M., Ramaekers F.C., Kuijpers H.J., Groenewoud J.S., Oosterhuis J.W. and Looijenga L.H. (1997). Nuclear lamin expression in normal testis and testicular germ cell tumours of adolescents and adults. *J. Pathol.* 182, 197-204.
- Mancini M.A., Shan B., Nickerson J.A., Penman S. and Lee W.H. (1994). The retinoblastoma gene product is a cell cycle-dependent, nuclear matrix-associated protein. *Proc. Natl. Acad. Sci. USA* 91, 418-422.
- Manilal S., Nguyen T.M., Sewry C.A. and Morris G.E. (1996). The Emery-Dreifuss muscular dystrophy protein, emerin, is a nuclear membrane protein. *Hum. Mol. Genet.* 5, 801-808.
- Maniotis A.J., Chen C.S. and Ingber D.E. (1997). Demonstration of mechanical connections between integrins, cytoskeletal filaments, and nucleoplasm that stabilize nuclear structure. *Proc. Nat. Acad. Sci. USA* 94, 849-854.
- Martelli A.M., Billi A.M., Gilmour R.S., Manzoli L., Di Primio R. and Cocco L. (1992). Mouse and human hemopoietic cell lines of erythroid lineage express lamins A, B and C. *Biochem. Biophys. Res. Commun.* 185, 271-276.
- Moir R.D., Montag-Lowy M. and Goldman R.D. (1994). Dynamic properties of nuclear lamins: lamin B is associated with sites of DNA replication. *J. Cell Biol.* 125, 1201-1212.
- Moir R.D., Spann T.P. and Goldman R.D. (1995). The dynamic properties and possible functions of nuclear lamins. *Int. Rev. Cytol.* 162B, 141-182.
- Morris G.E. and Manilal S. (1999). Heart to heart: from nuclear proteins to Emery-Dreifuss muscular dystrophy. *Human Mol. Genet.* 8, 1847-1851.
- Newport J.W., Wilson K.L. and Dunphy W.G. (1990). A lamin-independent pathway for nuclear envelope assembly. *J. Cell Biol.* 111, 2247-2259.
- Nickerson J.A. (1998). Nuclear dreams: the malignant alteration of nuclear architecture. *J. Cell Biochem.* 70, 172-180.
- Ohno M., Fornerod M. and Mattaj J.W. (1998). Nucleocytoplasmic transport: the last 200 nanometers. *Cell* 92, 327-336.
- Oyama T. (1989). A histopathological, immunohistochemical and ultrastructural study of intranuclear cytoplasmic inclusions in thyroid papillary carcinoma. *Virchows Arch.* 414, 91-104.
- Paddy M.R., Saumweber H., Agard D.A. and Sedat J.W. (1996). Time resolved, in vivo studies of mitotic spindle formation and nuclear lamina breakdown in *Drosophila* early embryos. *J. Cell Sci.* 109, 591-607.
- Paulin-Levasseur M., Blake D.L., Julien M. and Rouleau L. (1996). The MAN antigens are non-lamin constituents of the nuclear lamina in vertebrate cells. *Chromosoma* 104, 367-379.
- Pederson T. and Spann T.P. (1998). Preparation of nuclei from tissue and suspension cultures. In: *Cells: A Laboratory Manual*. Vol. 1. Spector D.L., Goldman R.D. and Leinwand L.A. (eds). Cold Spring Harbor Laboratory Press. Cold Spring Harbor, New York. pp 43.1-43.14.
- Pyrpasopoulou A., Meier J., Maison C., Simos G. and Georgatos S.D. (1996). The lamin B receptor (LBR) provides essential chromatin docking sites at the nuclear envelope. *EMBO J.* 15, 7108-7119.
- Rando O.J., Zhao K. and Crabtree G.R. (2000). Searching for a function for nuclear actin. *Trends Cell Biol.* 10, 92-97.
- Rosai J., Carcangiu M.L. and Delellis R.A. (1992). *Tumors of the thyroid gland*. Armed Forces Institute of Pathology. Washington.
- Sarria A.J., Lieber J.G., Nordeen S.K. and Evans R.M. (1994). The presence or absence of a vimentin-type intermediate filament network affects the shape of the nucleus in human SW-13 cells. *J. Cell Sci.* 107, 1593-1607.
- Sasseville A.M. and Langelier Y. (1998). In vitro interaction of the carboxy-terminal domain of lamin A with actin. *FEBS Lett.* 425, 485-489.
- Shu H.B. and Joshi H.C. (1995). Gamma-tubulin can both nucleate microtubule assembly and self-assemble into novel tubular structures in mammalian cells. *J. Cell Biol.* 130, 1137-1147.
- Spann T.P., Moir R.D., Goldman A.E., Stick R. and Goldman R.D. (1997). Disruption of nuclear lamin organization alters the distribution of replication factors and inhibits DNA synthesis. *J. Cell Biol.* 136, 1201-1212.
- Vickery A.L. Jr., Carcangiu M.L., Johannessen J.V. and Sobrinho-Simoes M. (1985). Papillary carcinoma. *Semin. Diagn. Pathol.* 2, 90-100.
- Viglietto G., Chiappetta G., Martinez-Tello F.J., Fukunaga F.H., Tallini G., Rigopoulou D., Visconti R., Mastro A., Santoro M. and Fusco A. (1995). RET/PTC oncogene activation is an early event in thyroid carcinogenesis. *Oncogene* 11, 1207-1210.
- Wilson K.L. (2000). The nuclear envelope, muscular dystrophy, and gene expression. *Trends Cell Biol.* 10, 125-129.
- Worman H.J., Yuan J., Blobel G. and Georgatos S.D. (1988). A lamin B receptor in the nuclear envelope. *Proc. Natl. Acad. Sci. USA* 85, 8531-8534.
- Wynford-Thomas D. (1997). Origin and progression of thyroid epithelial tumours: cellular and molecular mechanisms. *Horm. Res.* 47, 145-157.
- Yang L., Guan T. and Gerace L. (1997). Lamin-binding fragment of LAP2 inhibits increase in nuclear volume during the cell cycle and progression into S phase. *J. Cell Biol.* 139, 1077-1087.
- Ye Q. and Worman H.J. (1996). Interaction between an integral protein of the nuclear envelope inner membrane and human chromodomain proteins homologous to *Drosophila* HP1. *J. Biol. Chem.* 271, 14653-14656.
- Ye Q., Callebaut I., Pezhman A., Courvalin J.C. and Worman H.J. (1997). Domain-specific interactions of human HP1-type chromodomain proteins and inner nuclear membrane protein LBR. *J. Biol. Chem.* 272, 14983-14989.
- Ye Q., Barton R.M. and Worman H.J. (1998). Nuclear lamin-binding proteins. *Sub-Cellular Biochem.* 31, 587-610.